Journal of Crystal Growth 27 (1974) 118–125 © North-Holland Publishing Co.

DEFECTS IN EPITAXIAL MULTILAYERS*

I. MISFIT DISLOCATIONS

J. W. MATTHEWS and A. E. BLAKESLEE

IBM Thomas J. Watson Research Center, Yorktown Heights, New York 10598, U.S.A.

Received 6 March 1974; revised manuscript received 10 July 1974

Multilayers composed of many thin films of GaAs and $GaAs_{0.5}P_{0.5}$ were grown epitaxially on GaAs surfaces inclined at a few degrees to (001). Examination of the multilayers by transmission and scanning electron microscopy has revealed that the interfaces between layers were made up of large coherent areas separated by long straight misfit dislocations. The Burgers vectors of the dislocations were inclined at 45° to (001) and were of type $\frac{1}{2}a\ \langle 110 \rangle$. Dislocations in adjacent interfaces were usually not independent of one another. They often lay on the same slip plane and when this was so they were clearly products of the same source. The layer thickness at which misfit dislocations were formed was in satisfactory agreement with the predicted thickness. However, the fraction of the total misfit accommodated by dislocations (once the critical thickness for dislocation generation was passed) was much smaller than predicted. This large discrepancy seems to arise from difficulties associated with the creation of misfit dislocations. Although there are many processes which can impede dislocation generation, the most important one in $GaAs/GaAs_{0.5}P_{0.5}$ multilayers appears to be the impaction of dislocations on one glide plane against dislocations in another.

1. Introduction

The accommodation of misfit across the interface between an epitaxial film and its substrate has been considered by Frank and van der Merwe[1,2]). They show that a misfit smaller than about 7 percent will be accommodated by uniform elastic strain until a critical film thickness is reached. Thereafter, it is energetically favorable for misfit to be shared between dislocations and strain. Experimental tests of these predictions have been made on many bicrystals. In the majority of these tests the agreement between predictions and experiment has been satisfactory. However, in some the fraction of misfit accommodated by elastic strain has been larger than predicted[3–5]). The discrepancies between prediction and experiment in these systems are believed to result from difficulties associated with the generation of misfit dislocations[6]).

The aim of this paper is to describe a study of misfit accomodation in epitaxial multilayers. The multilayers were made by depositing a succession of gallium arsenide and gallium arsenide–phosphide films on a gallium arsenide substrate. All layers were single crystals in the orientation of their substrate. They were accurately planar and their thickness was uniform to within a few percent. They were prepared for the 'semiconducting superlattice' device proposed by Esaki and Tsu[7]).

* A summary of this work was presented at the Conference on Vapor Growth and Epitaxy, Jerusalem, May 1973.

2. Experimental details

Alternating layers of GaAs and $GaAs_{0.5}P_{0.5}$ were grown on GaAs substrates using the Ga–AsH_3–PH_3–HCl–H_2 vapor system. In this system GaCl is formed by reaction of Ga with HCl and transported by the H_2 carrier gas, with either AsH_3 or AsH_3+PH_3, into the deposition zone. Reactive deposition produces an epitaxial layer of GaAs or Ga(As,P) on the substrate surface. The details of the apparatus used to grow the alternating layers have been described elsewhere[8]). An important feature of it is the ability to inject PH_3 into the AsH_3 vapor stream so that there is little mixing of the AsH_3 and AsH_3+PH_3 pulses as they move to the deposition zone. However, some mixing is inevitable, and as a result of it, the interfaces between layers are not perfectly sharp.

The duration of the injection of PH_3 was controlled by a solenoid valve activated by an electronic timer. The relative thicknesses of the GaAs and Ga(As,P) layers could be adjusted by varying the ratio of the off to on times. However, the on and off times were equal in all specimens described here. This ensured that the thicknesses of the GaAs and Ga(As,P) layers were approximately equal. The multilayers contained either 60 or 120 layers and the layer thickness ranged from 75 to 700 Å. Layer thickness was determined from scanning electron micrographs of the multilayers viewed from the side or from the positions of satellite peaks in X-ray diffraction patterns[9]). The resolution limit of the scanning microscope was smaller than 150 Å. This resolution enables one to determine the wavelength, or repeat distance, in a multilayer made of GaAs and Ga(As,P) layers that are each about 75 Å in thickness. All layers with the exception of the thickest were grown in 1 sec. The injection time used for the thickest (700 Å) layers was 5 sec.

The GaAs substrate surfaces were chemically polished and were inclined at between 2° and 3° to (001). The rotation away from (001) was about a ⟨110⟩ axis in (001). The density of dislocations in the substrates was always less than $5 \times 10^4/\mathrm{cm}^2$ and usually less than $1 \times 10^4/\mathrm{cm}^2$. The wafer temperature during the deposition of the multilayers was 750 °C. An epitaxial GaAs layer 10 to 20 μm in thickness was grown on the substrate surface before the deposition of the alternating layers began. This layer was doped with between 10^{17} and 10^{18} sulphur atoms per cm^3. The multilayers were sometimes doped similarly.

Samples were prepared for transmission electron microscopy in the following way. Wafers were lapped on the substrate side to a total thickness of ~ 250 μm and cleaved into small squares so as to fit into the sample holder of the microscope. The multilayer side of each square was then attached to a thin glass cover slide with a methanol-insoluble grease. The slide was mounted vertically and a fine jet of a solution containing 15 drops of Br_2 in 100 ml of CH_3OH was directed against the center of the sample. This removed GaAs at approximately 12 μm/min and produced a polished surface. Etching was stopped as soon as a small hole appeared in the sample. Specimens were removed from the slide by dissolving the grease in trichlorethylene.

3. Observations

3.1. The geometry of misfit dislocations

Specimens composed of layers 75, 160, 350, 380, 440 and 700 Å in thickness were examined. Dislocations that accommodated part of the misfit between layers were found in specimens composed of 350, 380, 440, and 700 Å layers. However, they were not present in specimens composed of thinner layers. This means that the critical thickness for the generation of misfit dislocations lay somewhere between 160 and 350 Å.

Four misfit dislocations between 700 Å layers are seen in fig. 1. A feature of these and many of the other dislocations present to accommodate misfit between individual layers is that they are paired. The Bragg reflections responsible for image contrast in fig. 1. were $\bar{2}\bar{2}0$ in (a), 040 in (b), $\bar{2}20$ in (c) and 400 in (d). Two pairs of dislocations are visible in (a) and (c), the upper pair is visible in (b), and the lower one in (d). The invisibility of the lower pair of dislocations in (b) shows that the Burgers vectors of this pair lay in (010). If we assume[10]) that stable, complete dislocations in GaAs or Ga(As,P) have Burgers vectors of type $\frac{1}{2}a\langle 110\rangle$ then the Burgers vectors of the lower pair were either $\pm\frac{1}{2}a\,[101]$ or $\pm\frac{1}{2}a\,[10\bar{1}]$. The Burgers vectors of the upper pair were either $\pm\frac{1}{2}a\,[011]$ or $\pm\frac{1}{2}a\,[01\bar{1}]$. All these possible Burgers vectors are inclined at 45° to (001) and at 60° to the dislocation lines. The misfit accommodated by dislocations with this geometry is only half that accommodated by edge dislocations with Burgers vectors in (001). The dislocations in fig. 1 are thus inefficient misfit dislocations. However, they are the most efficient complete misfit dislocations that can be made by glide to the interface on {111} slip planes. The dislocations are straight because the lines of intersection of {111} slip planes and the interface are straight.

Dislocations similar to those in fig. 1 have been found in silicon doped by diffusion[11]), in GaAs–Ga(As,P) samples[12]), and in deposits of one fcc metal on another[13,14]). The fact that the dislocations in fig. 1 go out of contrast in pairs rather than singly is consistent with the hypothesis (proved below) that paired dislocations have antiparallel Burgers vectors.

The separation, S, of paired dislocations was found, in the majority of cases, to obey the following relation:

$$S = h \cot 55^\circ, \tag{1}$$

where h is the thickness of individual GaAs or Ga(As,P) layers, and 55° is the angle between {111} slip planes and the (almost) (001) interface between layers. Paired misfit dislocations that did not obey eq. (1) had spacings that were either three or five times the spacing given by

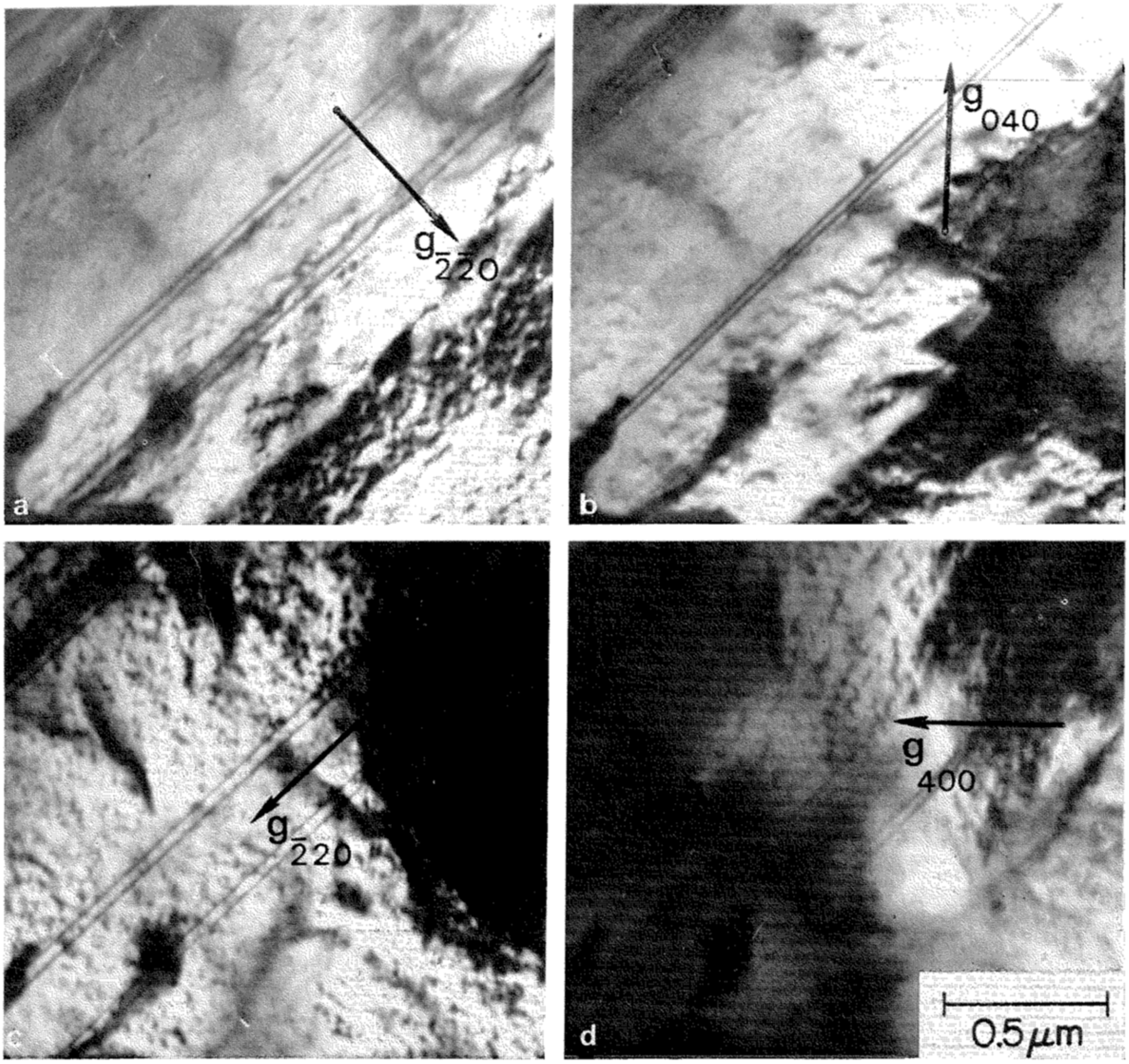

Fig. 1. Four micrographs of a specimen composed of 700 Å layers. The layers were almost perpendicular to the incident electron beam. The reflections responsible for the image contrast were $\bar{2}\bar{2}0$ in (a), 040 in (b), $\bar{2}20$ in (c) and 400 in (d).

eq. (1). These results suggest that paired dislocations lay on the same {111} plane and in interfaces that were either one, three or five layers apart.

Paired dislocations separated by three 350 Å layers are seen in the micrographs in fig. 2. An important feature revealed by this figure is that paired dislocations are joined to one another. They are portions of the same dislocation line. This means that paired dislocations have antiparallel Burgers vectors.

Although many of the misfit dislocations in samples composed of layers 350 Å or more in thickness were paired, there were many others arranged in parallel and uniformly spaced arrays. Portions of two arrays in the specimen made up of 700 Å layers are seen in fig. 3 (a, b and c). Some of the properties of the dislocation arrays are listed below.

(i) The dislocation lines were parallel to the lines of intersection of {111} slip planes and the interface. As the interface plane was close to (001) this means that the dislocation lines were approximately parallel to the [110] and [$\bar{1}$10] directions in the (001) plane.

(ii) The Burgers vectors of the dislocations were of type $\frac{1}{2}a\langle 110\rangle$ and were inclined at 45° to (001). This result follows from fig. 3 (b) if one assumes that the Burgers vectors of stable, complete dislocations in fcc crystals are of type $\frac{1}{2}a\langle 110\rangle$.

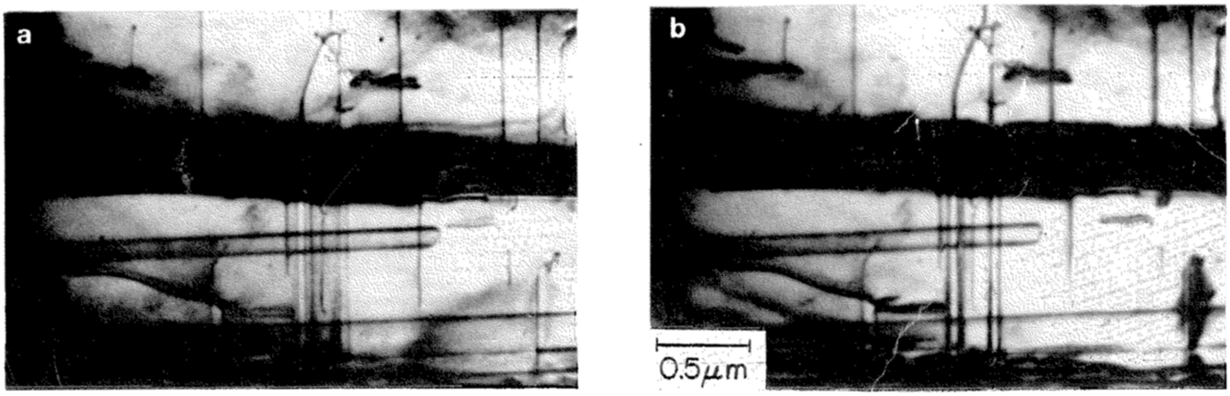

Fig. 2. Successive micrographs which show the removal of paired misfit dislocations. The dislocations were separated by three 350 Å layers and they lay on the same (111) glide plane. The layers were approximately perpendicular to the incident electron beam.

(iii) The average separation of adjacent parallel dislocations obeyed $S = h \cot 55°$.
(iv) Members of an array lay in the same or in nearby {111} planes. This result is suggested by (iii) and confirmed by fig. 3 (c) which was recorded after the sample had been tilted to bring a set of {111} planes parallel to the incident beam. It can be seen that this tilt brought the members of an array vertically above one another.
(v) Most arrays terminated against other arrays. An example of this is present in fig. 3.
(vi) The end of the visible array in fig. 3 (b) shows that the dislocations in the array were joined to one another in pairs. Examination of both ends of arrays has revealed that they consist of single dislocations that bend back and forth as illustrated in fig. 4. This means that the Burgers vectors of the parallel portions of arrays alternate in sign as shown in fig. 5.
(vii) The area occupied by individual arrays was often hundreds of square microns. The arrays in fig. 3 extended beyond the borders of the figure and, although we do not have direct evidence for this, there is little doubt that they extended to interfaces above and below those present in the thinned sample. Evidence that arrays often involved almost all the interfaces present in a multilayer is provided by micrographs like the one in fig. 6. This figure is a scanning electron image of an etched {110} cleavage surface perpendicular to the multilayer plane. The layer thickness was 440 Å. The horizontal dark and light lines are images of individual layers. The rows of pits that pass obliquely

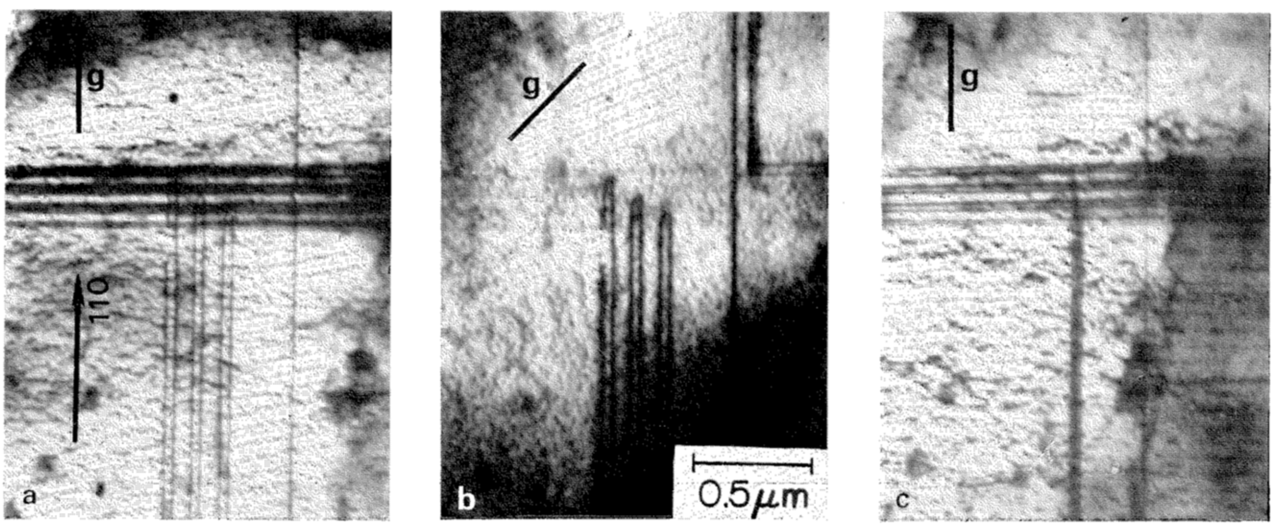

Fig. 3. Two arrays of misfit dislocations in the specimen composed of 700 Å layers. The layers were approximately perpendicular to the incident electron beam in (a) and (b). The specimen was tilted in (c) so as to view (111) planes edge on.

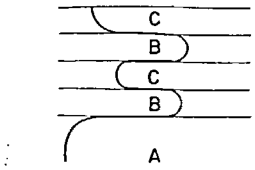

Fig. 4. An array of misfit dislocations.

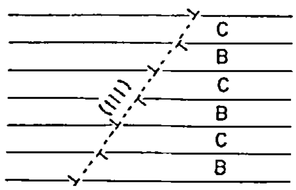

Fig. 5. A section through an array of misfit dislocations.

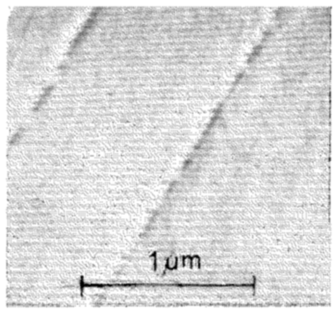

Fig. 6. Scanning electron micrograph of a multilayer seen from the side. The thickness of the layers was 440 Å. Pits mark the emergence points of dislocations in arrays on (111).

across the figure mark the emergence points of dislocations arranged in arrays on two parallel {111} planes. In addition to showing the extent of arrays this figure reveals that dislocations are sometimes absent from a few of the interfaces present.

3.2. Elimination of misfit dislocations

Creation of misfit dislocations has not been observed, but the reverse process has. Figs. 2 (a) and 2 (b) are successive electron micrographs of the sample composed of 350 Å layers. The parallel lines near the center of each micrograph are misfit dislocations that have antiparallel Burgers vectors and lines that are separated by three layers. The micrographs reveal the removal of short lengths of these dislocations by the motion of the threading dislocation that connects them.

If paired dislocations are separated by a single layer they can be destroyed by a process which is slightly different from that in fig. 2. Dislocations in adjacent interfaces can move towards one another and cancel. If

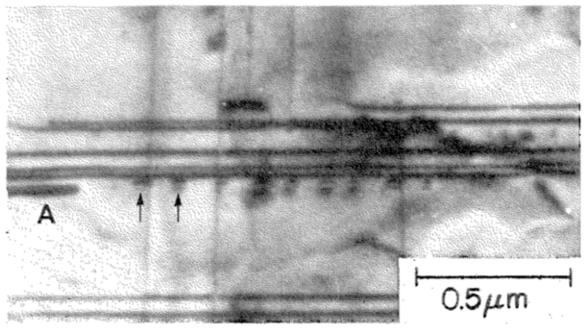

Fig. 7. Dislocation loops left after paired dislocations had annihilated one another at several points along their length. Layer thickness = 350 Å.

the dislocations lie on the same {111} plane this motion is by glide. If they lie on adjacent or nearby {111} planes their motion involves climb as well as glide. A train of dislocation loops left after cancellation had occurred at various points along the length of a pair of dislocations (A) with antiparallel Burgers vectors are present in fig. 7. Two of the loops are arrowed. The thickness of individual layers in fig. 7 was 350 Å.

The elimination of misfit dislocations from the specimen composed of 350 Å layers suggests that diffusion reduced the misfit between adjacent layers sufficiently for misfit dislocations to be unstable. (By this we mean that diffusion raised h_c from below 350 Å to above.) This is discussed further in 4.2 and 4.3.

3.3. Misfit accommodated by dislocations

The misfit accommodated by dislocations with the geometry described in 3.1 is

$$\delta_{BC} = b/2d, \tag{2}$$

where b is the strength of the dislocations, and d the average distance between dislocation lines in the same interface. Measurements of d in the specimen composed of 700 Å layers showed that $\delta_{BC} \approx 10^{-4}$. This is less than one percent of the misfit between GaAs and $GaAs_{0.5}P_{0.5}$; it is compared with the predicted value for δ_{BC} in 4.4.

4. Discussion

4.1. Dislocation formation

4.1.1. *Dislocation arrays*

One mechanism for formation of arrays is clear from fig. 4. A substrate dislocation with suitable Burgers

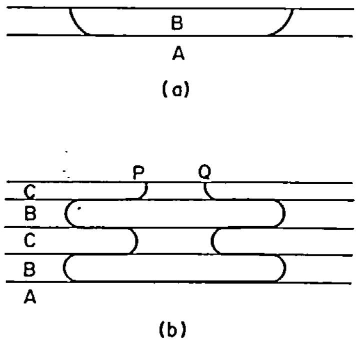

Fig. 8. Mechanism for creation of dislocation arrays.

vector is replicated in the deposit. This dislocation glides back and forth under the influence of coherency strain and generates interfacial dislocations as it does so.

Although this mechanism gives arrays with the geometry of those observed it is unable to explain the number of arrays present. The dislocations that terminate on the substrate surface can account for less than one percent of the observed arrays. From this we may conclude that many threading dislocations are created during layer growth. Comparison of the number of dislocations that terminate on the substrate surface with the number that terminate on the surface of the multilayer confirms this conclusion. The density of dislocations in the substrate surface was $< 5 \times 10^4/\text{cm}^2$. The density in the multilayer surface was $\sim 10^8/\text{cm}^2$.

A mechanism for the creation of pairs of threading dislocations, and for conversion of these threading dislocations into dislocation arrays, is illustrated in fig. 8. The misfit strain in the first B layer results in the nucleation of a dislocation half-loop on a {111} plane. This loop grows by glide to make a pair of threading dislocations and a length of misfit dislocation line in the AB interface [fig. 8(a)]. The growth of additional B and C layers is accompanied by back and forth motion of the threading dislocations to make misfit dislocations in BC and CB interfaces [fig. 8(b)]. The process is terminated if dislocations like P and Q in fig. 8(b) meet during the growth of the layer in which they lie and annihilate one another. This is an improbable event, however. This is because[15]) it is energetically favorable for δ_{AB} to exceed the dislocation content of the final BC interface when the stress-free lattice parameters of the substrate (A) and C layers are equal.

The nucleation of half-loops like the one in fig. 8(a) has been discussed elsewhere[16]). It will not begin until the thickness of the first layer is large enough for it to contain a half-loop stable under the misfit strain.

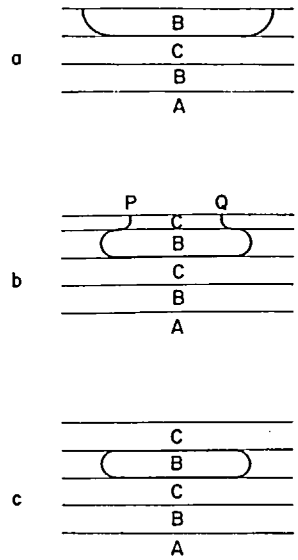

Fig. 9. Mechanism for formation of paired dislocations.

The number of threading dislocations made as in fig. 8 will only be significant if the misfit strain is large enough for dislocation nucleation to be probable at the temperature of film growth. The calculations of Frank[17]) and Hirth[18]) suggest that the 1.8% misfit between GaAs and $GaAs_{0.5}P_{0.5}$ is sufficient for this purpose.

4.1.2. *Paired dislocations*

Although paired dislocations are made when one of the loops in an array (see fig. 4) travels further than the remainder, this may not be the only mechanism for their generation. An alternative process is shown in fig. 9. A half-loop similar to that in fig. 8 (a) is created in a layer other than the first. During the growth of the next layer portions of the loop labelled P and Q move towards one another and annihilate. Annihilation is probable because, as has been shown elsewhere[15]), it is energetically favorable for the dislocation content of the final interface to exceed that of the penultimate or semifinal one.

4.2. Effects of diffusion

A realistic diffusion coefficient for GaAs–Ga(As,P) at 750 °C is believed to be 10^{-15} cm^2/sec. If we assume this value then for all specimens except the one composed of 700 Å layers the diffusion distance $[2\sqrt{(Dt)}]$ was $\sim$ 6 Å at the end of the growth of a single layer, was $\lesssim$ 70 Å after the growth of a multilayer, and was $\sim$ 130 Å by the time specimens were examined.

4.3. Critical thickness for the formation of misfit dislocations

Interface structure in multilayers can be predicted from the forces on dislocation lines[19]). Two of the important forces are F_ε, the force exerted by the misfit strain, and F_l, the tension in the dislocation line. If the elastic constants of B and C are equal and isotropic, and $h_B = h_C$, then

$$F_\varepsilon = \frac{2G(1+\nu)}{(1-\nu)}\, bh\varepsilon \cos\lambda. \tag{3}$$

G is the shear modulus of B and C, ν is the Poisson ratio and λ is the angle between the slip direction and that direction in the film plane which is perpendicular to the line of intersection of the slip plane and the interface. The tension in the dislocation line is approximately

$$F_l = \frac{Gb^2}{4\pi(1-\nu)}\left(1-\nu\cos^2\alpha\right)\left(\ln\frac{h}{b}+1\right), \tag{4}$$

where α is the angle between the dislocation line and its Burgers vector.

The maximum value of the strain is $\varepsilon_{max} = \frac{1}{2} f$. If $F_{\varepsilon_{max}}$, the value of F_ε at ε_{max}, is less than $2F_l$ then threading dislocations will have geometry similar to (a) in fig. 10 and the interfaces between layers will be coherent. If $F_{\varepsilon_{max}} = 2\,F_l$, threading dislocations will have the geometry shown by (b). If $F_{\varepsilon_{max}} > 2\,F_l$, dislocations will move and assume the geometry of (c). This motion reduces ε and destroys the coherence of the interfaces between layers. The layer thickness at which $F_{\varepsilon_{max}} = 2\,F_l$ is

$$h_C = \frac{b}{2\pi f}\,\frac{(1-\nu\cos^2\alpha)}{(1+\nu)\cos\lambda}\left(\ln\frac{h_C}{b}+1\right). \tag{5}$$

h_C for GaAs–$GaAs_{0.5}P_{0.5}$ (where $\nu = \frac{1}{3}$, $b = 4$ Å, $\cos\alpha = \frac{1}{2}$, $\cos\lambda = \frac{1}{2}$, and $f = 0.018$) is $\sim$ 250 Å. Thus, the presence of misfit dislocations in interfaces between 350, 380, 440 and 700 Å layers (see 3.1) is expected. Escape of misfit dislocations during examination of 350 Å layers (see 3.2) is also not surprising. Diffusion after layer growth (see 4.2) would be expected to increase h_C from $\sim$ 250 Å to roughly 350 Å.

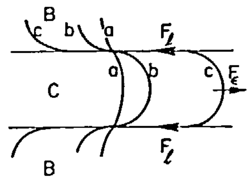

Fig. 10. Threading dislocations in coherent (a), critical (b), and incoherent (c) multilayers.

It is perhaps worth emphasizing that the calculations made above hold for *all* threading dislocations. It does not matter whether they are made by replication of dislocations present in the substrate or result from nucleation processes like the one illustrated in fig. 8.

The values of h_C predicted by eq. (5) is four times as great as the critical thickness expected in a system composed of a single epitaxial film on a substrate of infinite thickness. Half of this factor of four arises from the fact that the elastic misfit strain in a multilayer is shared between all layers. Half the layers are compressed and the other half are stretched. The remainder of the factor of four arises because the motion of a dislocation like that in fig. 10 makes two misfit dislocations. Migration of a threading dislocation in a specimen composed of a thin film on a thick substrate makes only one.

4.4. Relaxation of misfit strain

In ideal circumstances, the motion of a dislocation like (c) in fig. 10 reduces ε so as to keep $F_\varepsilon = 2F_l$. The misfit accommodated by dislocations when balance is maintained is

$$\delta_{BC} = f - \frac{b(1-\nu\cos^2\alpha)}{\pi h\,(1+\nu)\cos\lambda}\left(\ln\frac{h}{b}+1\right). \tag{6}$$

The value of δ_{BC} predicted by this equation for h = 700 Å is $\sim 10^{-2}$. This is about one hundred times the observed value (see 3.3). Discrepancies of this magnitude have been found in other systems and are believed to result from processes that impede relaxation of misfit strain[6]). Examples of these processes are the Peierls–Nabarro stress, the barrier to the nucleation of dislocations, and the interaction between dislocations.

The effect of the Peierls–Nabarro stress on the relaxation of misfit strain in semiconductors has been discussed elsewhere[16]). It is important when the substrate temperature and density of threading dislocations are low. The substrate temperature (750 °C) and the density of threading dislocations (10^8/cm^2) in the GaAs-Ga (As,P) multilayers suggest that the influence of the Peierls–Nabarro stress in these samples was small. Indeed, if it were the only impediment to dislocation formation, δ_{BC} would be expected to approach its optimum value [eq. (6)] in the time taken to grow a single GaAs or Ga(As,P) layer[16]).

The observation that most arrays of misfit dislocations were terminated by impaction against arrays on intersecting planes (see fig. 3) suggest that interaction between existing misfit dislocations, coupled with the barrier to the nucleation of new ones[17,18]), was largely responsible for the low value of δ_{BC}.

5. Final remarks

The multilayers described in this paper were prepared by CVD. It would be imprudent to suggest that all features of CVD multilayers would be present in specimens made by LPE or other techniques. However, there are some properties of CVD multilayers that one might expect to be quite general. The layer thickness at which the formation of misfit dislocations with the geometry described above is expected to begin is independent of preparation technique. Nucleation of dislocation half-loops is expected in all multilayers where growth temperature and misfit strain are suitably large. However, the misfit strain required for dislocation nucleation is influenced by surface steps, inclusions, and other defects that cause localized high stresses. The concentration and effectiveness of these stress raisers may depend on preparation technique. Processes that hinder the elongation of misfit dislocations are found in all systems. However, the magnitude of the effects they produce are known to vary from one epitaxial system to another[16]).

As its title implies, this paper is the first of a series of articles on defects in multilayers. Part II will be concerned with dislocation pile-ups and cracks formed in order to relieve elastic stresses present as a result of the misfit between the multilayer taken as a whole and its substrate. Part III will describe how multilayers free of misfit dislocations, threading dislocations, pile-ups, slip lines and cracks can be prepared.

Acknowledgements

We would like to thank B. K. Bischoff for his help with the growth of multilayers and with the preparation of samples for microscopy. Scanning electron micrographs were taken by C. G. Bremer, and the measurement of layer spacing by the X-ray satellite technique was performed by J. Angilello.

References

1) F. C. Frank and J. H. van der Merwe, Proc. Roy. Soc. (London) A **198** (1949) 216.
2) J. H. van der Merwe, J. Appl. Phys. **34** (1963) 117; J. H. van der Merwe, in: *Single Crystal Films* (Pergamon, New York, 1964) p. 139.
3) B. Borie, C. J. Sparks and J. V. Cathcart, Acta Met. **10** (1962) 691.
4) U. Gradmann, Ann. Physik **17** (1966) 91.
5) J. W. Matthews and E. Klokholm, Mater. Res. Bull. **7** (1972) 213.
6) N. Cabrera, Mem. Sci. Rev. Met. **62** (1965) 205.
7) L. Esaki and R. Tsu, IBM J. Res. Develop. **14** (1970) 61.
8) A. E. Blakeslee, J. Electrochem. Soc. **118** (1971) 1459.
9) A. Segmüller and A. E. Blakeslee, J. Appl. Cryst. **6** (1973) 19.
10) F. C. Frank and J. F. Nicholas, Phil. Mag. **44** (1953) 1213.
11) J. Washburn, G. Thomas and H. J. Queisser, J. Appl. Phys. **35** (1964) 1090.
12) M. S. Abrahams, J. R. Weisberg, C. J. Buiocchi and J. Blanc, J. Mater. Sci. **4** (1969) 223.
13) J. W. Matthews, Phil. Mag. **13** (1966) 1207.
14) J. W. Matthews and W. A. Jesser, Acta Met. **15** (1967) 595.
15) J. W. Matthews and A. E. Blakeslee, IBM Research Report RC 3854, May, 1972.
16) J. W. Matthews, S. Mader and T. B. Light, J. Appl. Phys. **41** (1970) 3800.
17) F. C. Frank, in: *Proc. Symp. on the Plastic Deformation of Crystalline Solids* (Carnegie Inst. of Technology, Pittsburgh, 1950) p. 89.
18) J. P. Hirth, *Relation between Structure and Strength in Metals and Alloys* (H. M. Stationery Office, London, 1963) p. 218.
19) W. A. Jesser and J. W. Matthews, Phil. Mag. **15** (1967) 1097.